
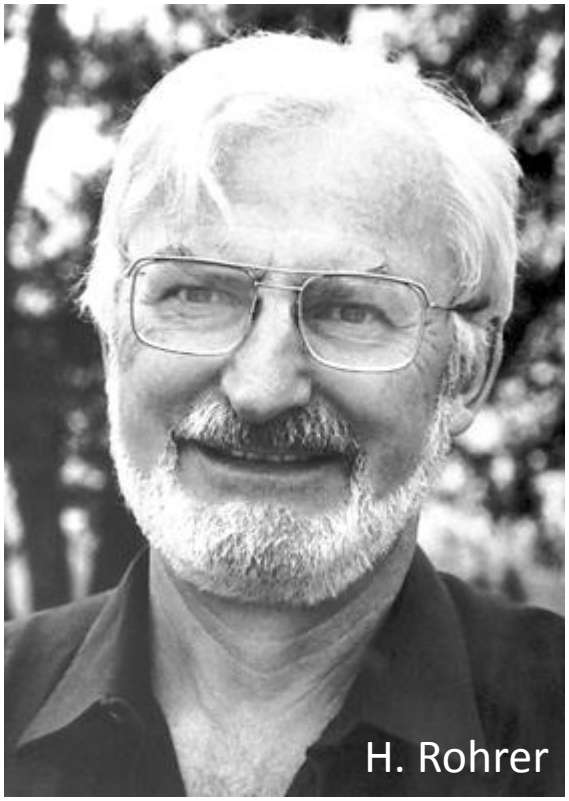


**Nobel price in physics 1986 for Binnig and Rohrer (shared with Ruska)** *"for their design of the scanning tunneling microscope"*.

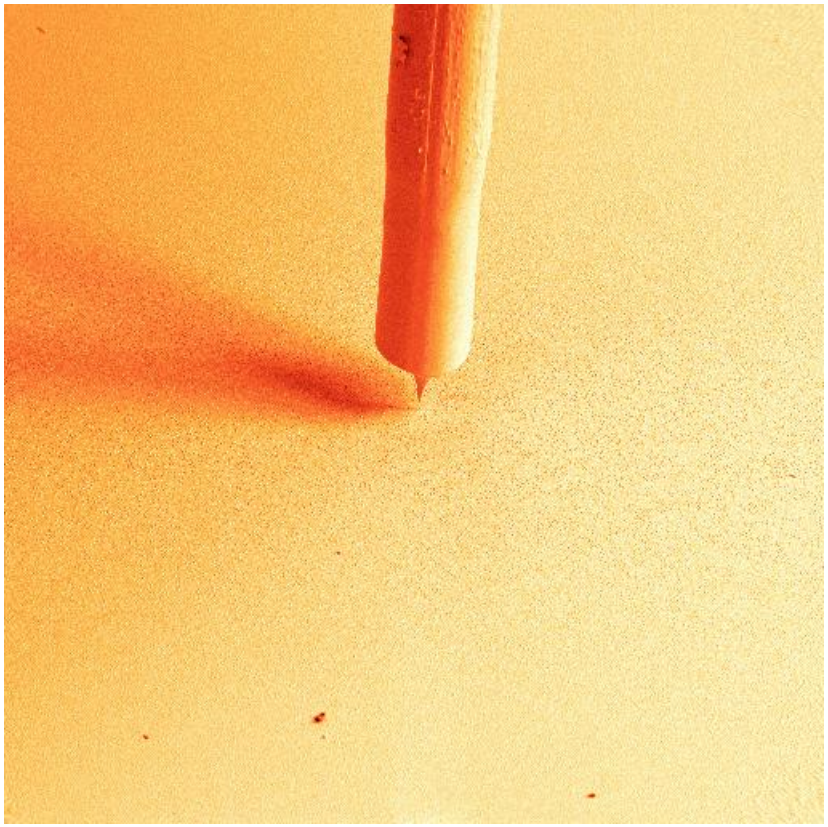

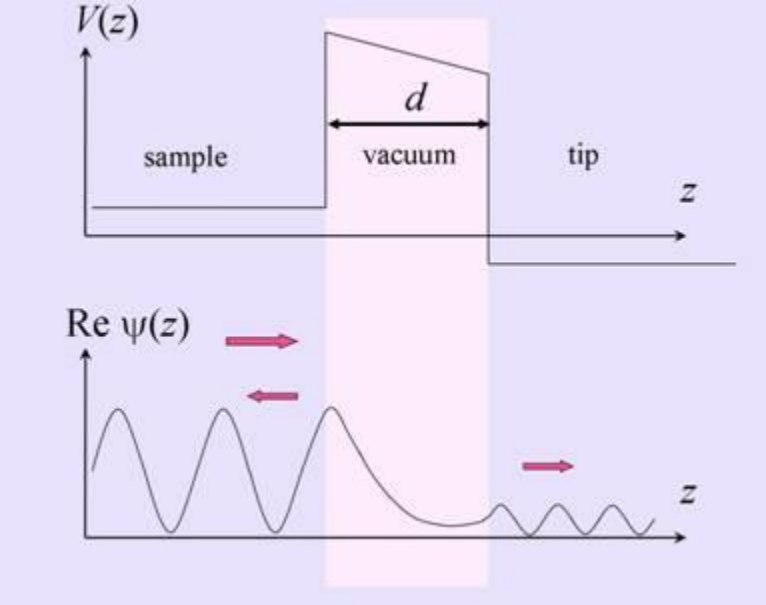


$$I \propto e^{-2\kappa d}$$

# Schema zur Besetzung von Bändern

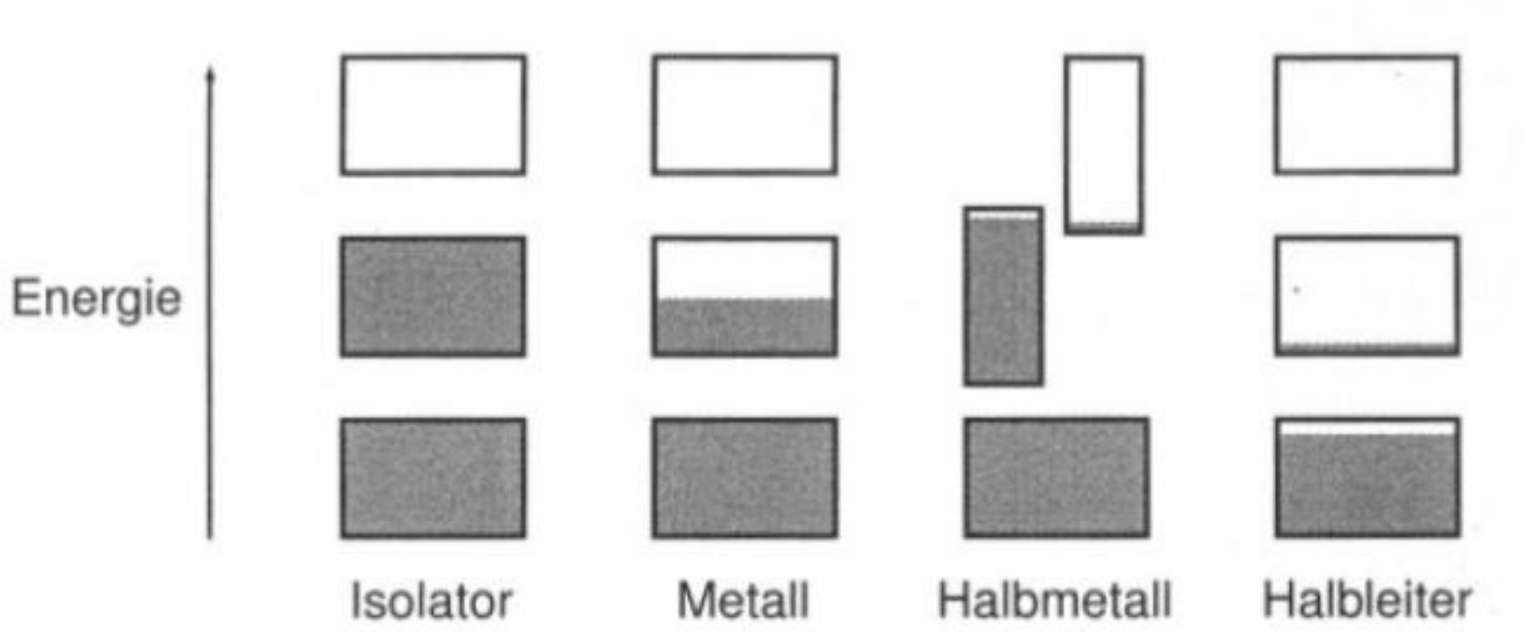


**Bild 7.1:** Schematische Darstellung der Besetzung erlaubter Energiebänder durch Elektronen für Isolator, Metall, Halbmetall und Halbleiter. Die Vertikalausdehnung der Rechtecke kennzeichnet die erlaubten Energiebereiche, die schattierten Flächen die mit Elektronen besetzten Bereiche.

# Band structure of Aluminium

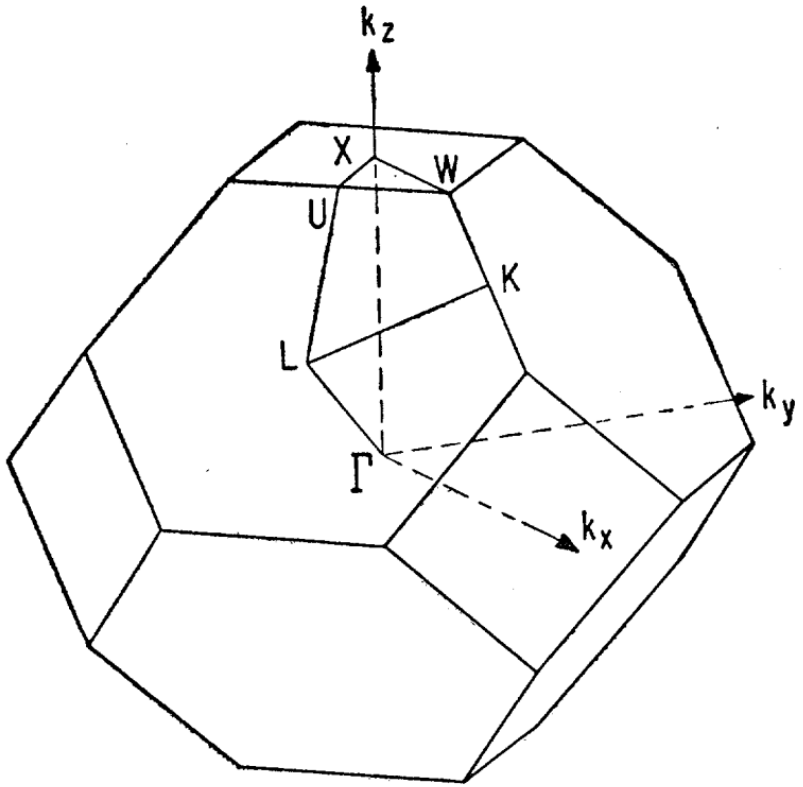


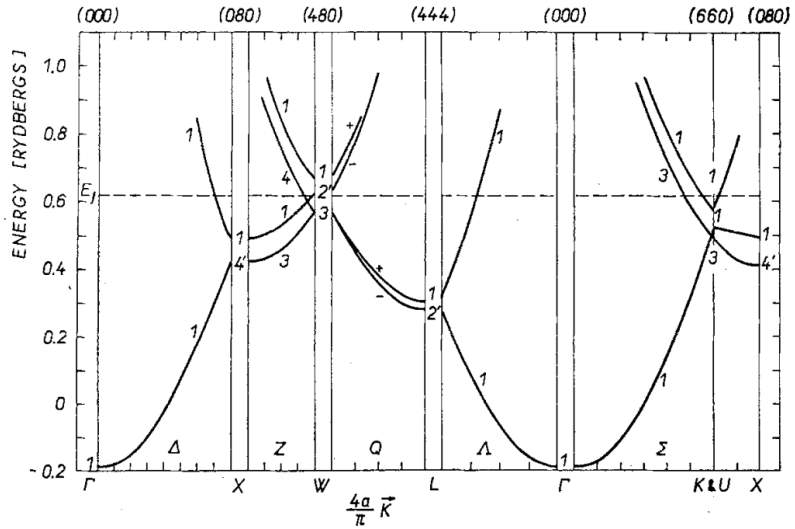


Fig. 2. Energy bands in directions of high symmetry.

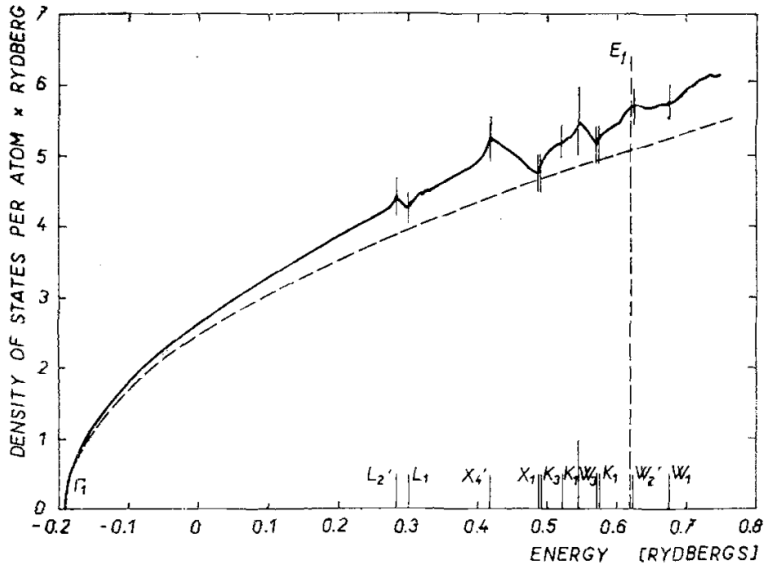


Fig. 3. The density of states. _____ present, _ _ _ _ _ free electron approximation.

# Band structure of copper

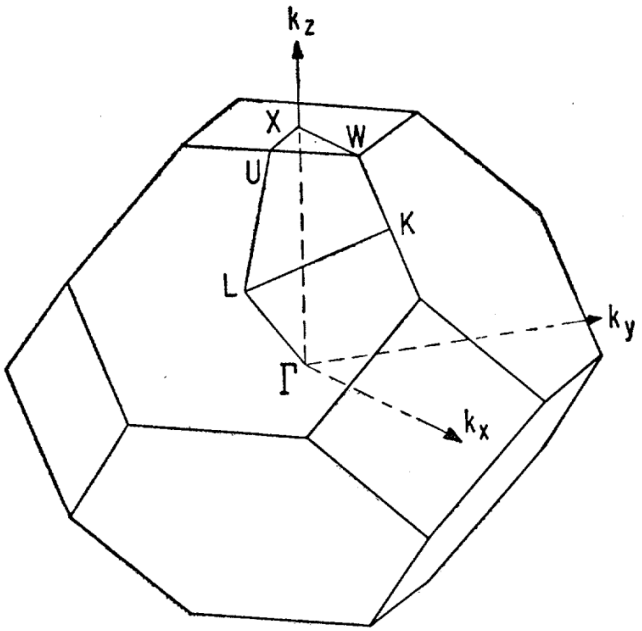


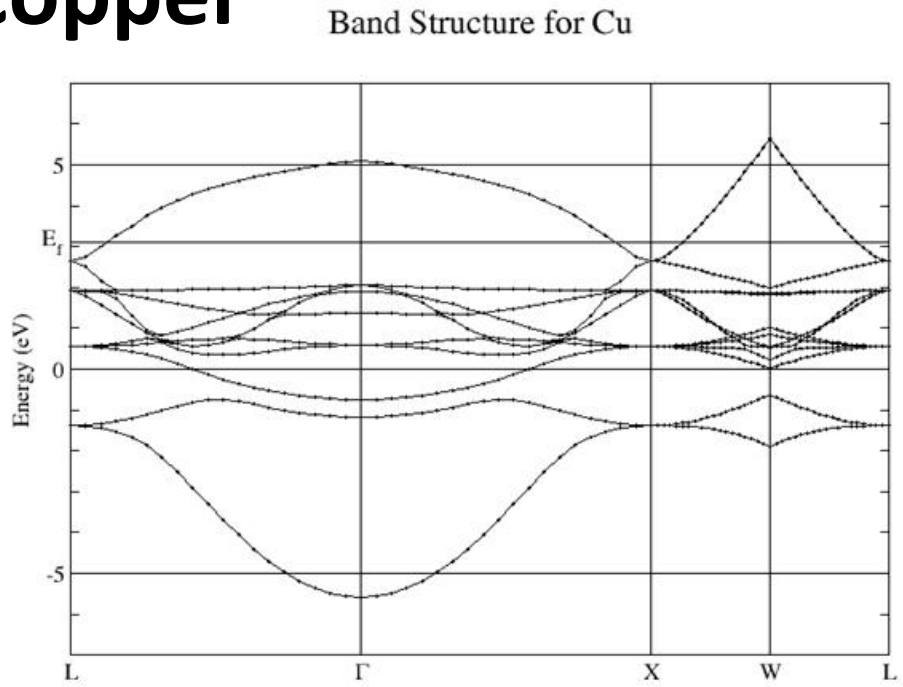


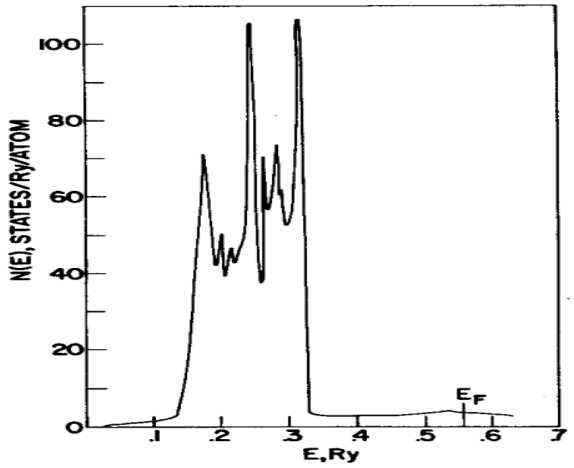

# Tersoff-Haman Theory for Au(110)- 2x1 and 3x1

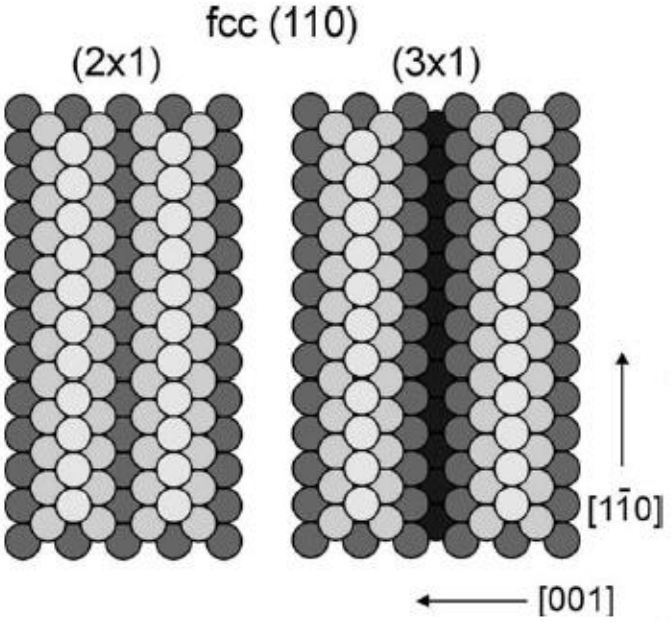


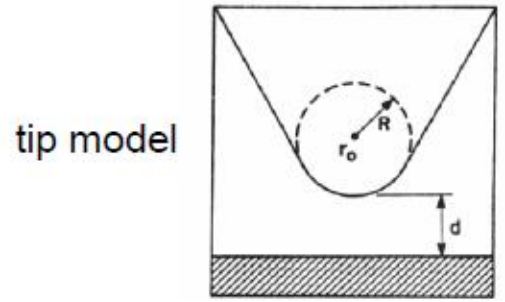


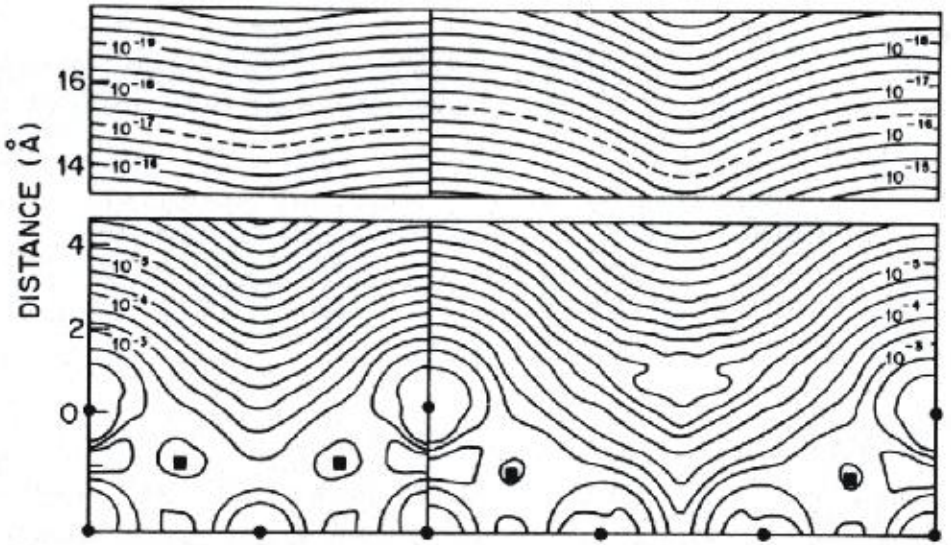


experiment: corrugation 0.45 Å (2x1) and 1.4 Å (3x1) with identical tip.

theory: R = 9Å, d= 6 Å, such that corrugation 0.45 Å for 2x1. This Implies a corrugation of 1.4 Å for the 3x1

FIG. 3. Calculated $\rho(\mathbf{r}, E_F)$ for Au(110) 2 × 1 (left) and 3 × 1 (right) surfaces. This figure shows (1$\bar{1}$0) plane through outermost atoms. Positions of nuclei are indicated by circles (in plane) and squares (out of plane). Contours of constant $\rho$ are labeled in units of a.u.$^{-3}$eV$^{-1}$. Note break in vertical distance scale. Assuming a 9 Å tip radius in the *s*-wave tip model, the center of curvature of the tip is calculated to follow the dashed line. (From Ref. 15.)

Fig. 25

# Atomic Resolution on Dense-Packed Surfaces

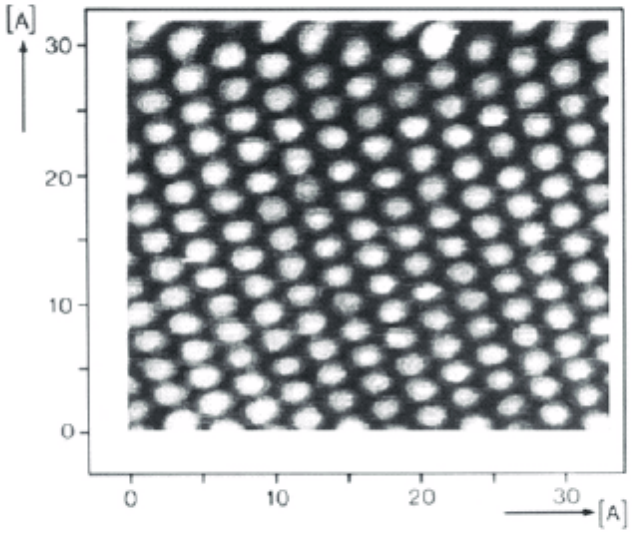


FIG. 1. Grey scale representation of an STM image of the clean Al(111) surface (34×34 Å$^2$, corrugation amplitude 0.3 Å, $V_t = -50$ mV, $I_t = 6$ nA).

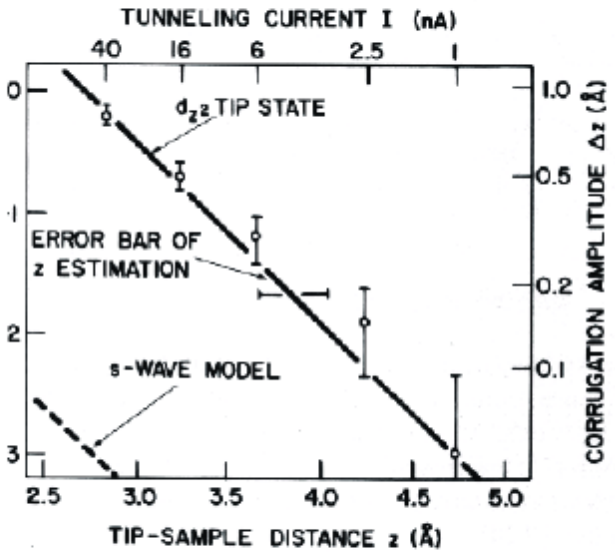


**Fig. 7.10.** Interpretation of the STM corrugation observed on Al(111). The predicted corrugation amplitude with a $d_{z^2}$ tip state, solid curve, agrees well with the experimental data from Wintterlin et al. (1989), circles with error bars. The parameters of the theoretical curve are taken from a first-principle calculation of Al(111) surface, Wang et al. (1981). The tip-sample distance is defined as the distance from the plane of the top-layer nuclei of the sample to the center of the apex atom of the tip [7.24]

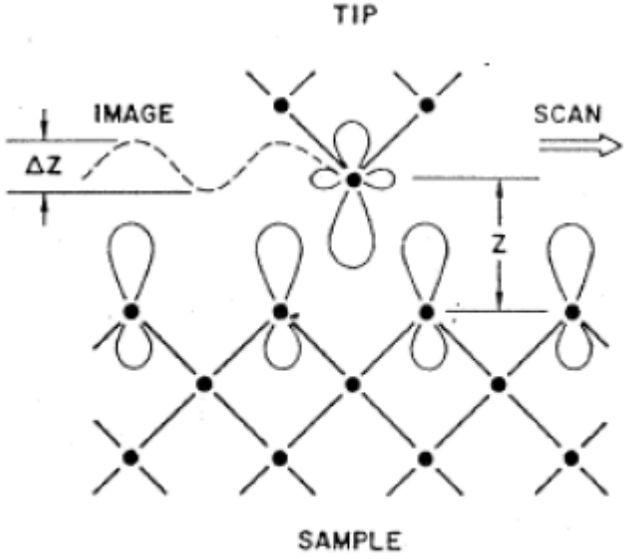


Fig. 26

# Piezo-Effekt

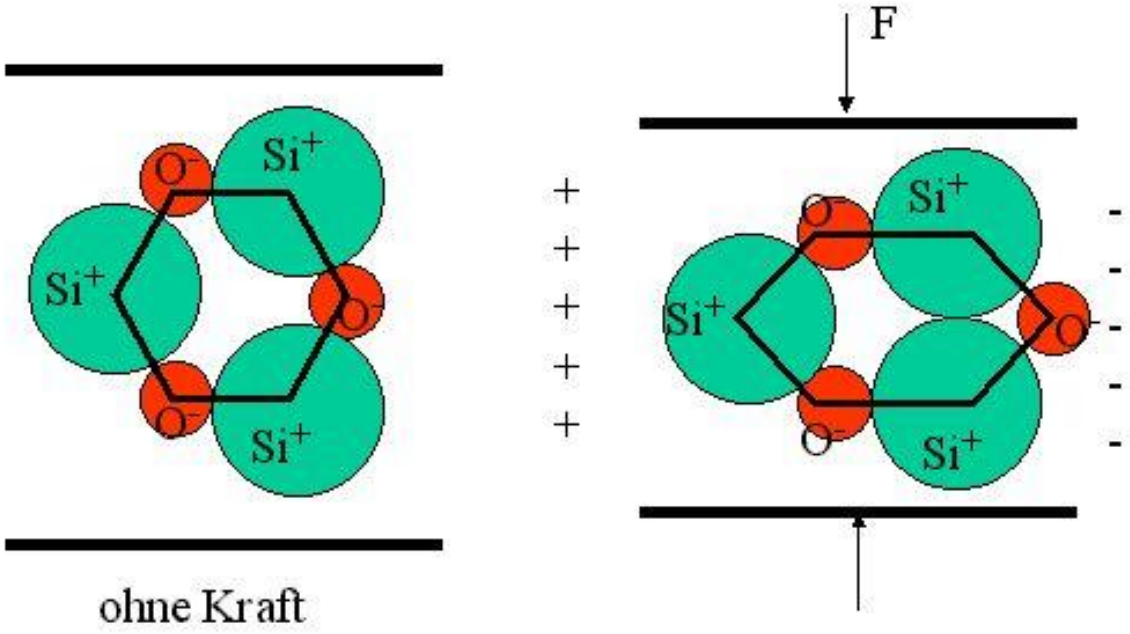


ohne Kraft

Netto-Dipolmoment !

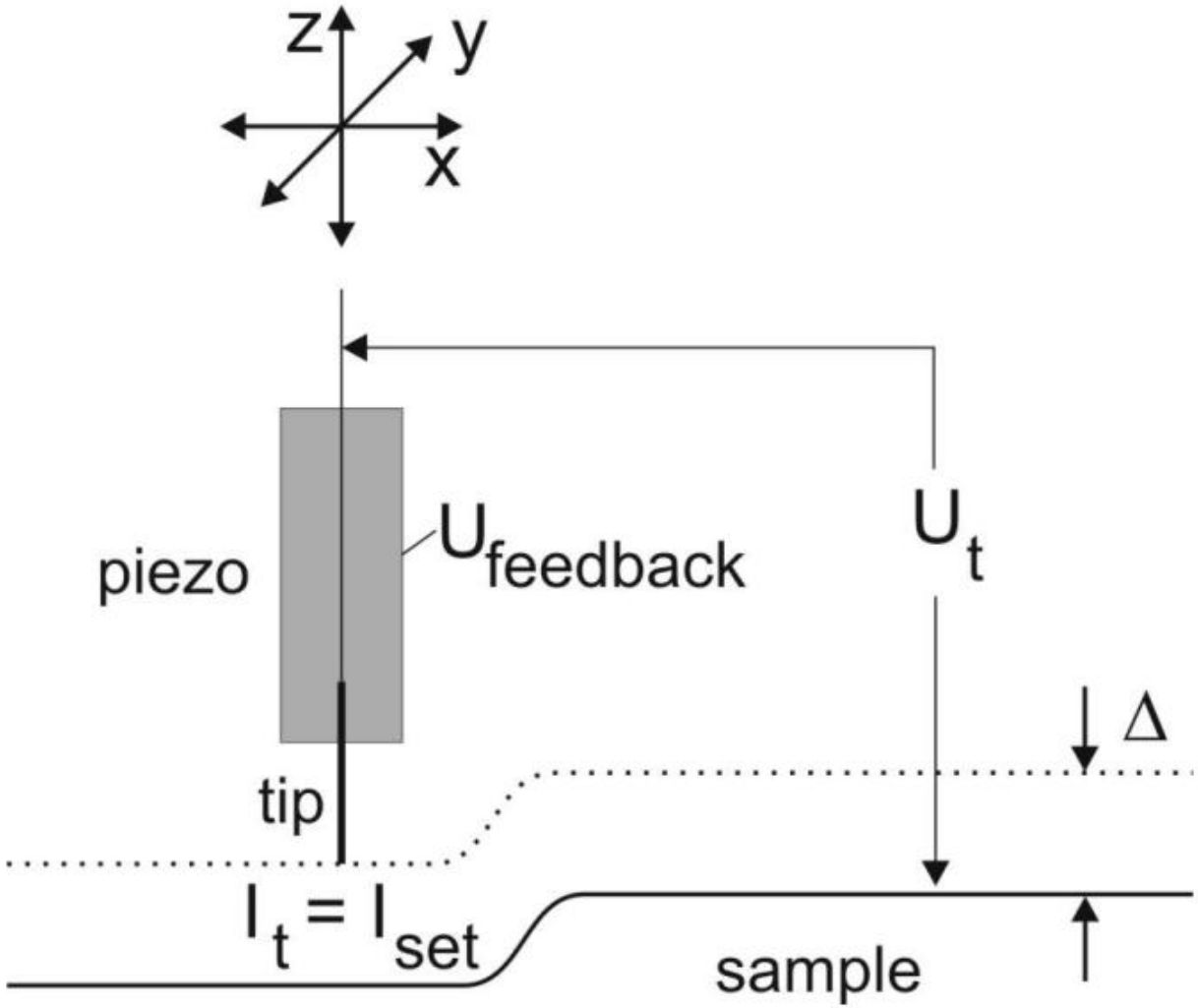
z
y
x
piezo
$U_{feedback}$
$U_t$
Δ
tip
$I_t = I_{set}$
sample

# Beetle STM

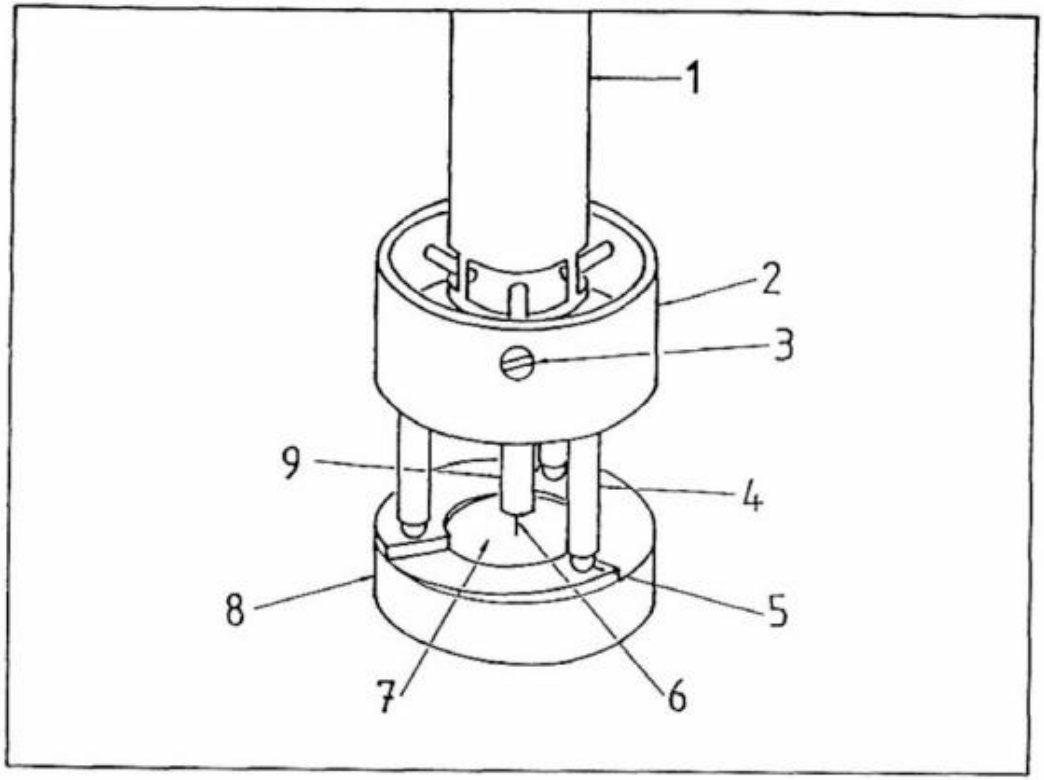


**Rastertunnelmikroskop:** Perspektivische Ansicht des entwickelten Rastertunnelmikroskops. 1 Halterohr, 2 Mikroskopkörper, 3 Halteschraube, 4 Rasterbein, 5 Stahlkugel, 6 Spitze, 7 Probe, 8 Rampenprobenhalter, 9 Z-Piezo.

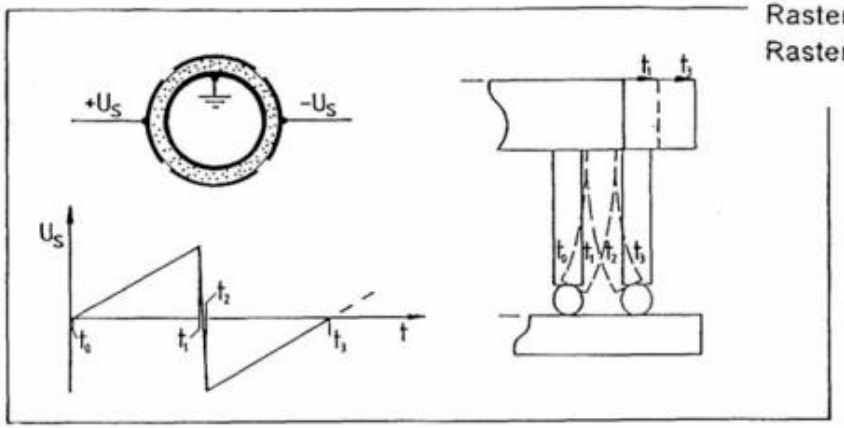


**Mikroskopbewegung:** Durch Anlegen eines Sägezahnimpulses $U_s$ an zwei gegenüberliegende Elektrodenflächen bewegt sich das Mikroskop wie rechts gezeigt einen "Schritt".

# Si(111) – 7x7 Rekonstruktion

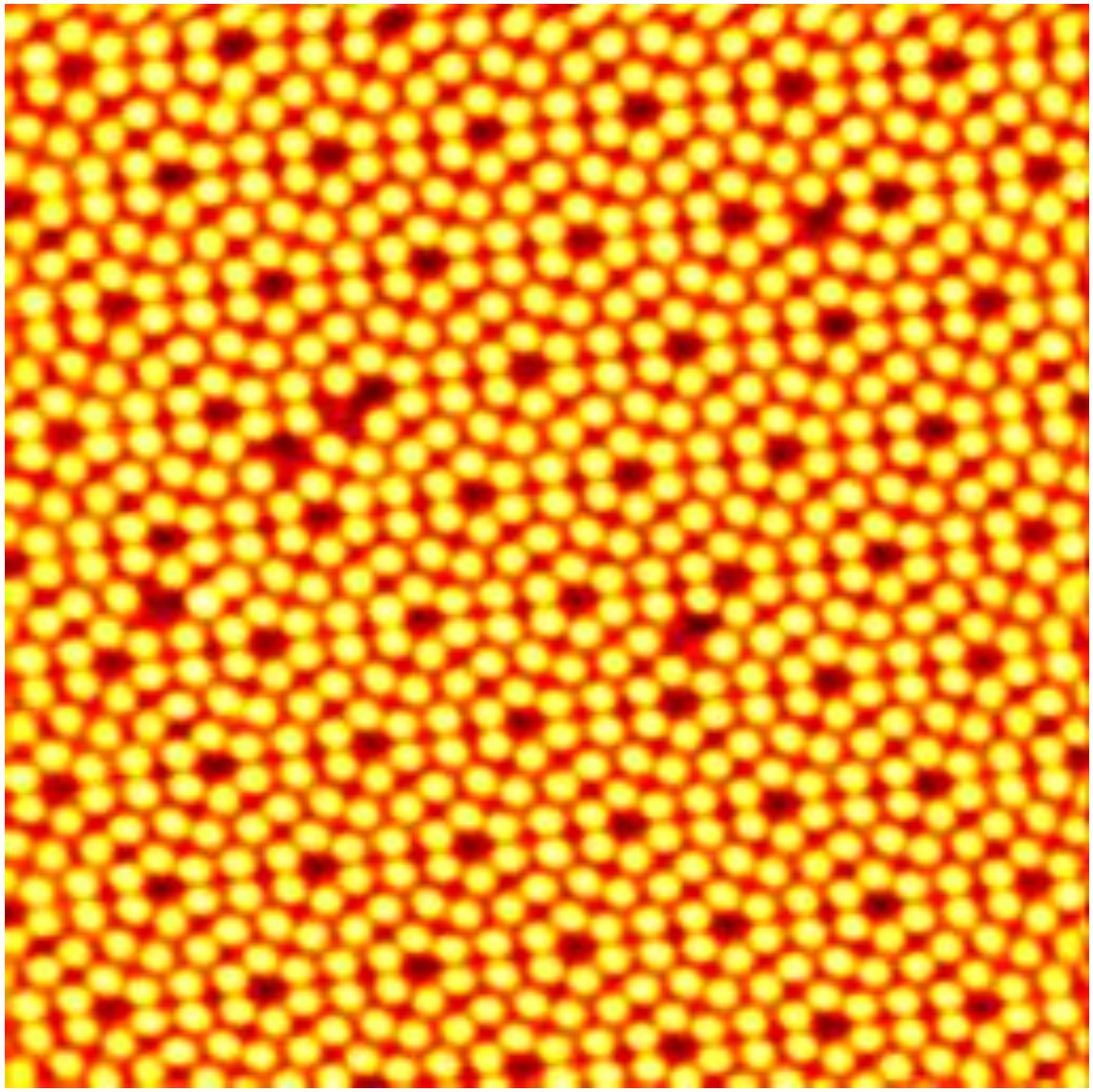

# Rekonstruktion von Halbleiteroberflächen: Si(111) – (7x7)

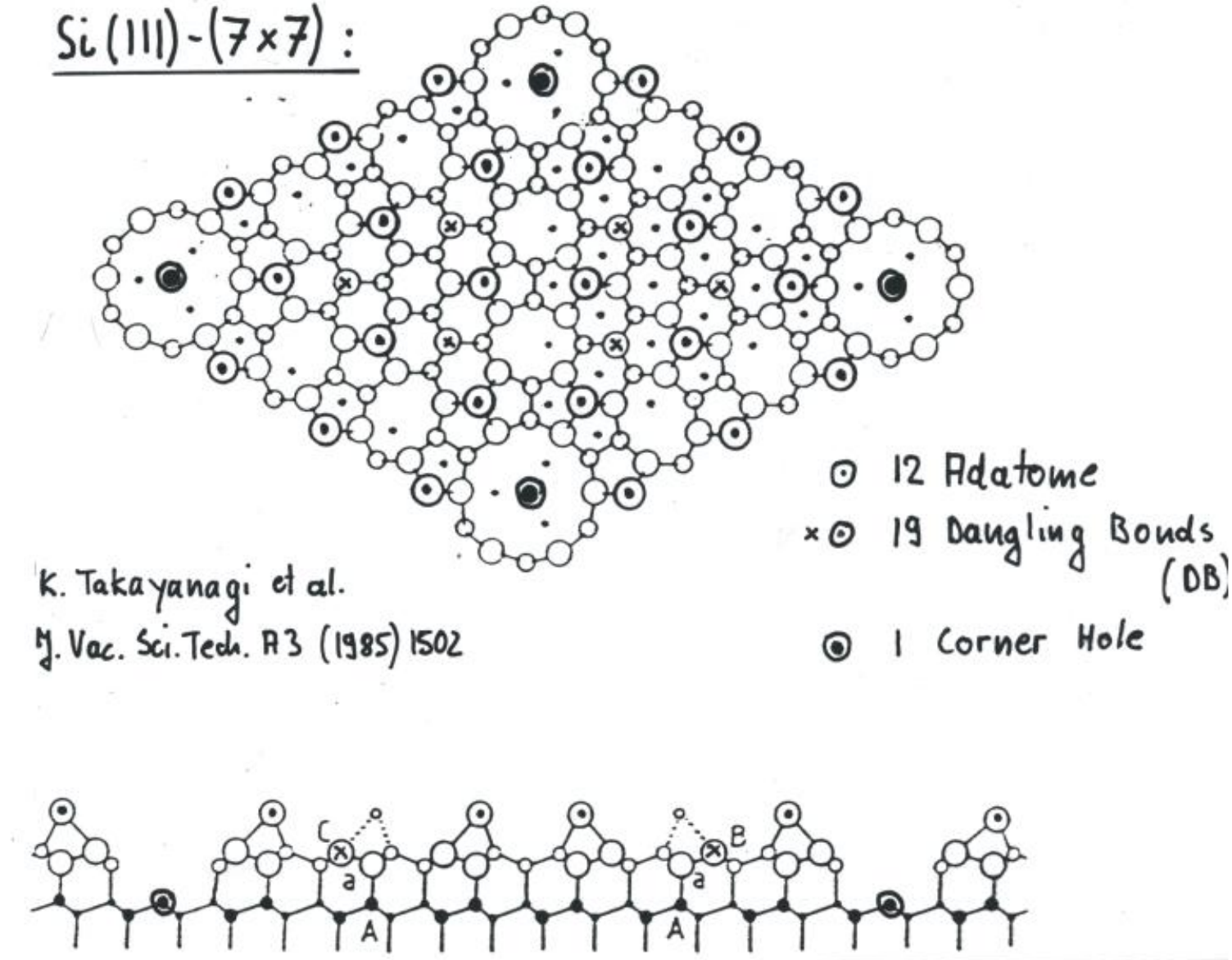

# Chemischer Kontrast für PtRh-Legierung ((111)-Oberfläche))

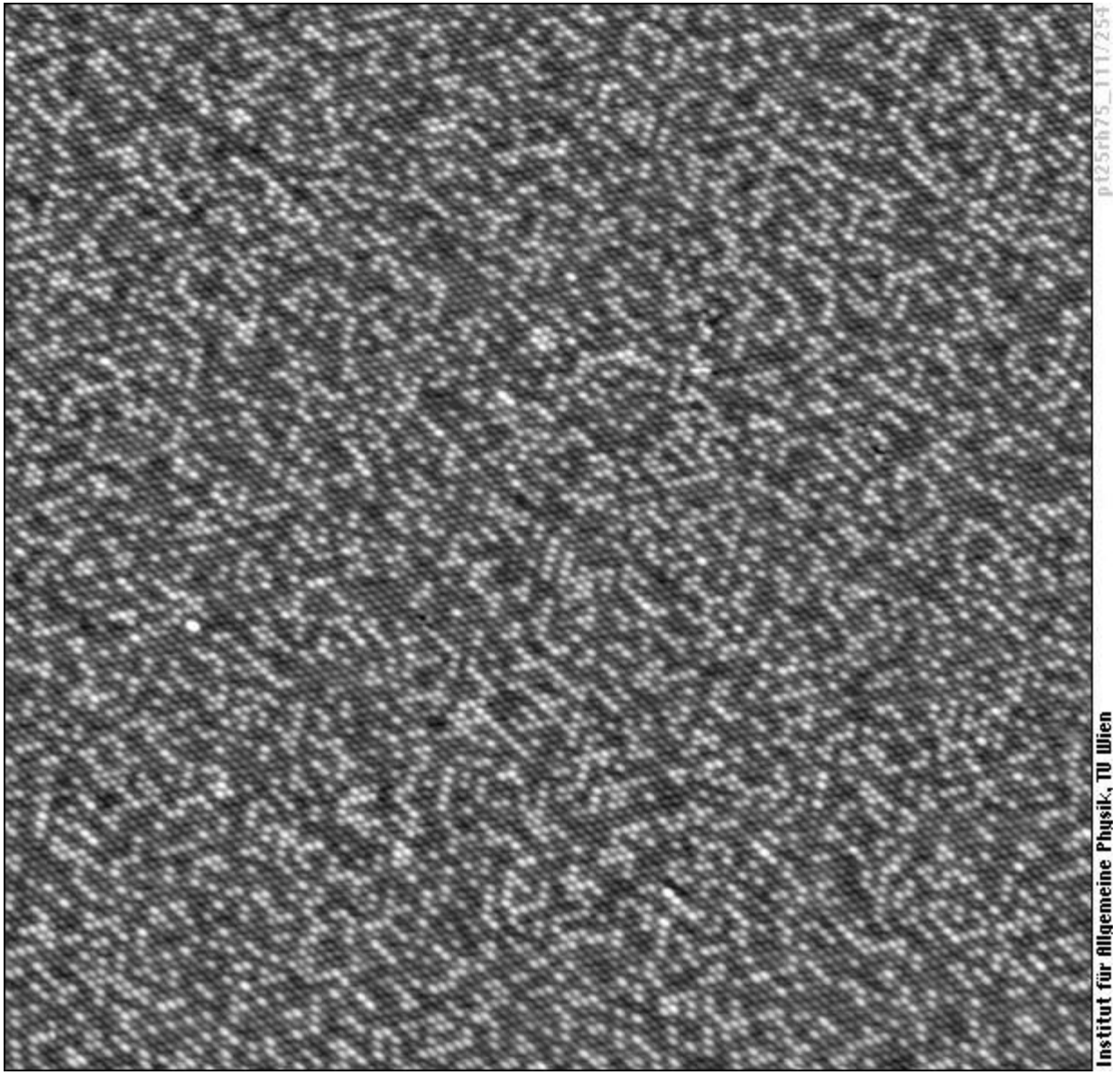

# Spitzenherstellung

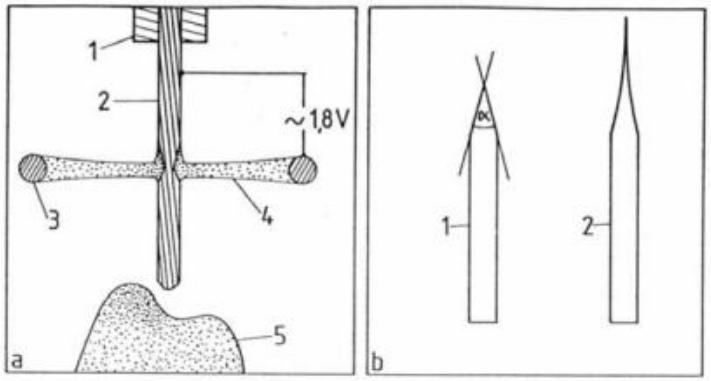


**Ätzverfahren und Spitzenform:** Abbildung a zeigt den schematischen Aufbau der Ätzanordnung. 1 Drahthalterung, 2 Wolframdraht, 3 Platindrahtschlaufe, 4 Elektrolyt, 5 Schaum. Abbildung b zeigt links eine günstige und rechts eine weniger günstige Spitzenform.

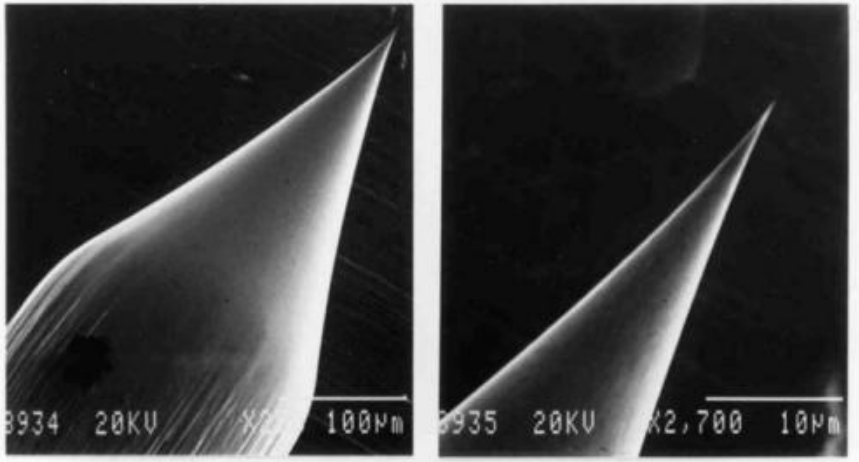


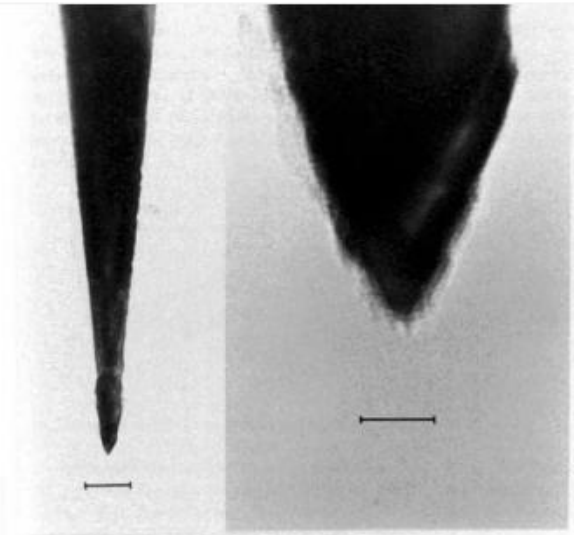

Abbildung 15: TEM-Aufnahmen einer typischen STM-Spitze. Die Markierungen entsprechen links 100 nm und rechts 10 nm.

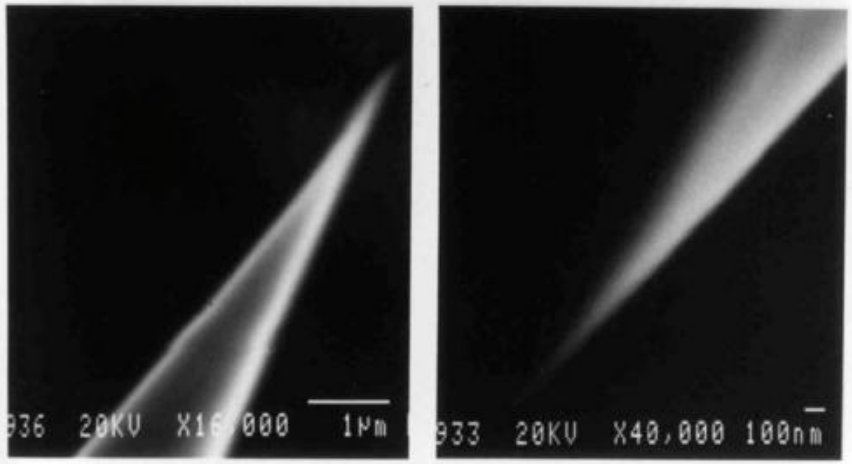


Abbildung 14: SEM-Aufnahmen einer typischen STM-Spitze mit zunehmender Vergrößerung. Strukturen unterhalb von 100 nm sind offensichtlich nicht mehr aufzulösen. (Rechts unten ist die Spitze um 180° gedreht.)

# Faltung von Spitzenform und Topographie: In Situ Spitzenformung

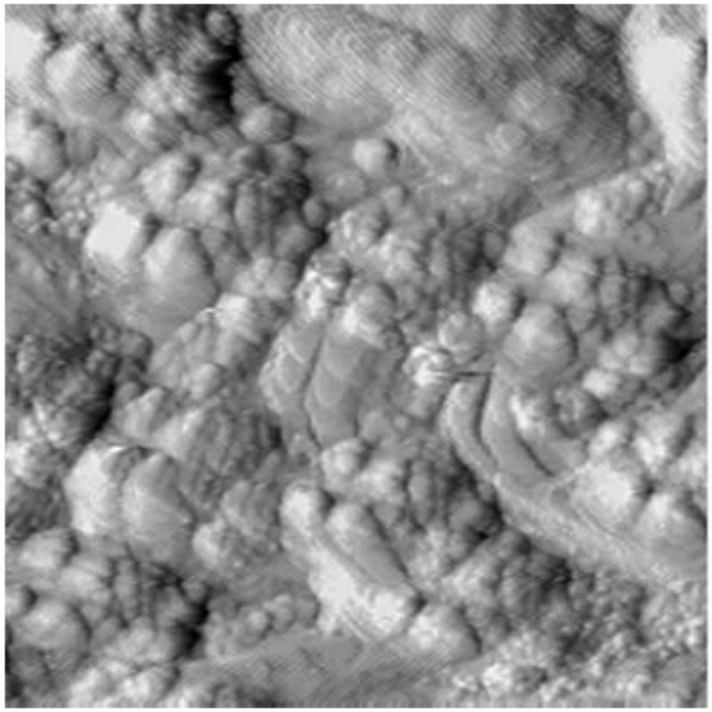

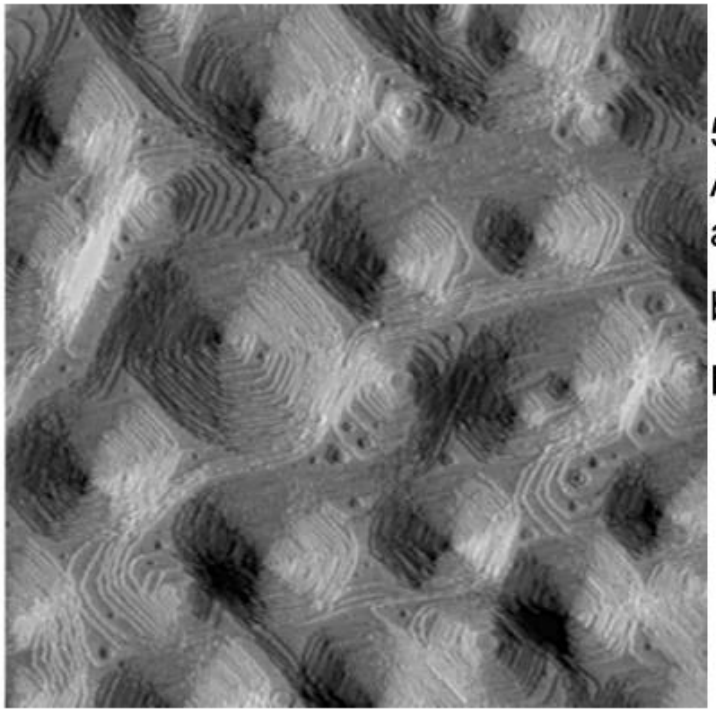

50 ML durch 600 eV Ar Ionenbeschuss abgetragen

bei 625 K

Rasterweite 1650Å

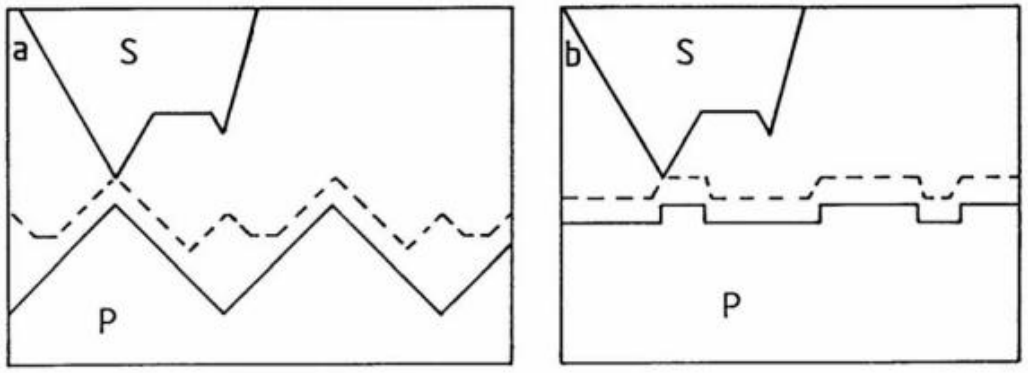


**Abb. 20. Abbildungseigenschaften und Probenrauhigkeit:** Gestrichelt eingetragen ist der Weg des äußersten Endes der Spitze, der maßgebend für die gemessene Morphologie ist. (a) rauhe Probe, (b) relativ glatte Probe

# Faltung von Spitzenform und Topographie: Tip Switch

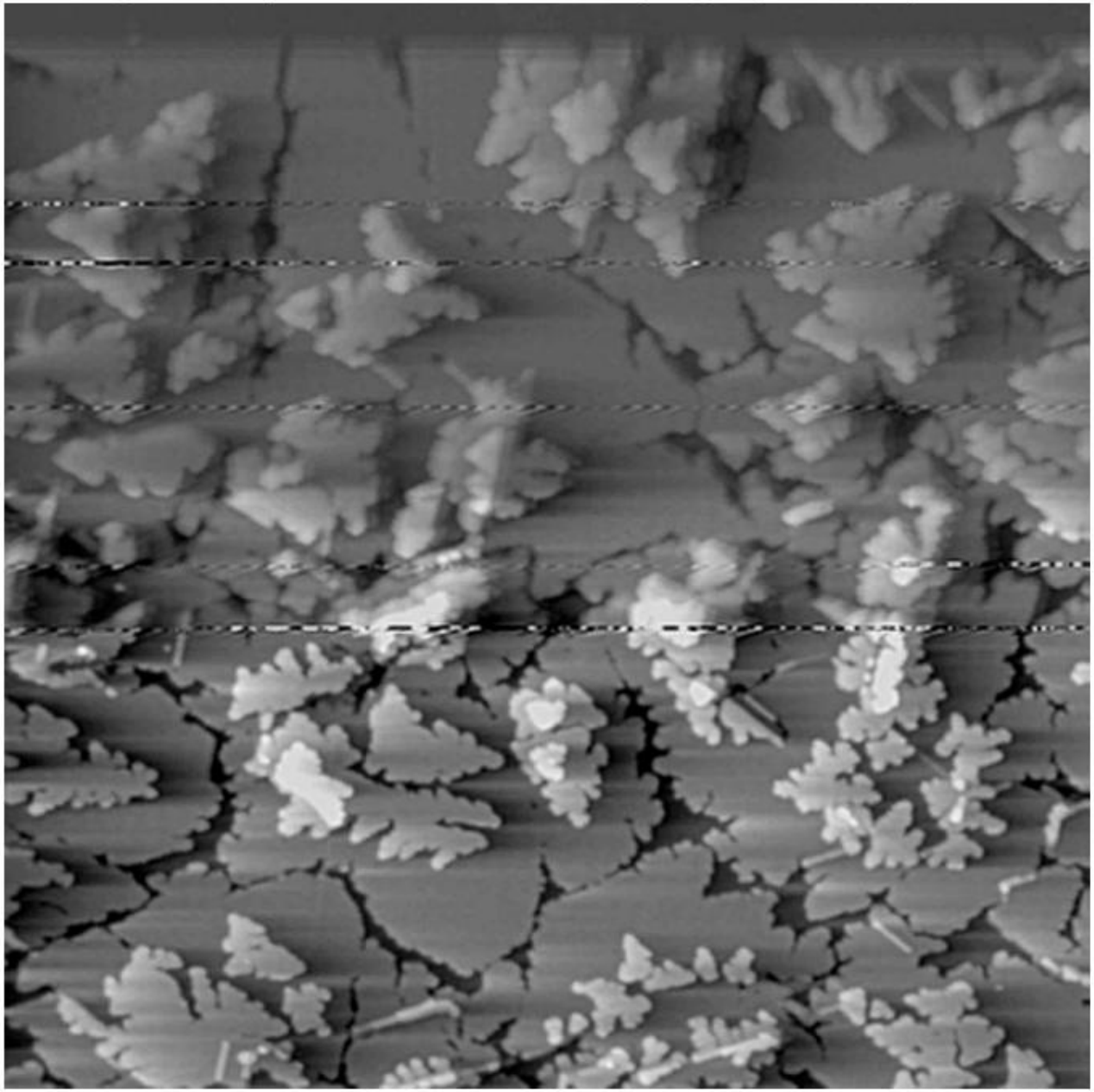

# STM Theorie

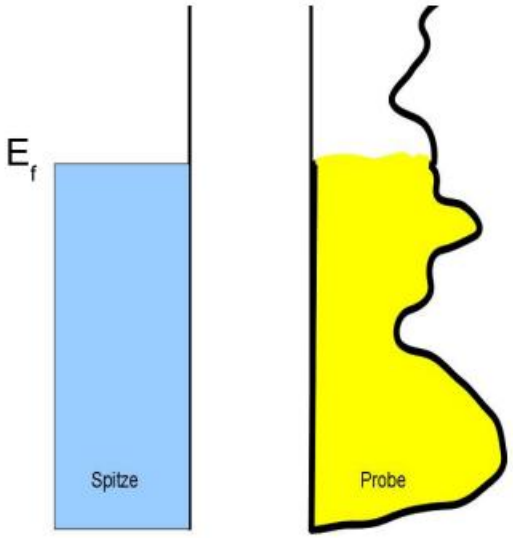


T=0, U=0

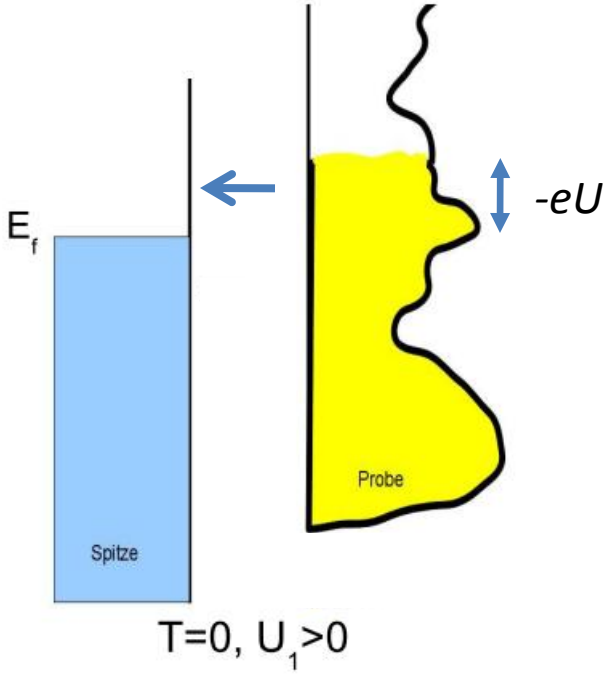


T=0, $U_1$>0

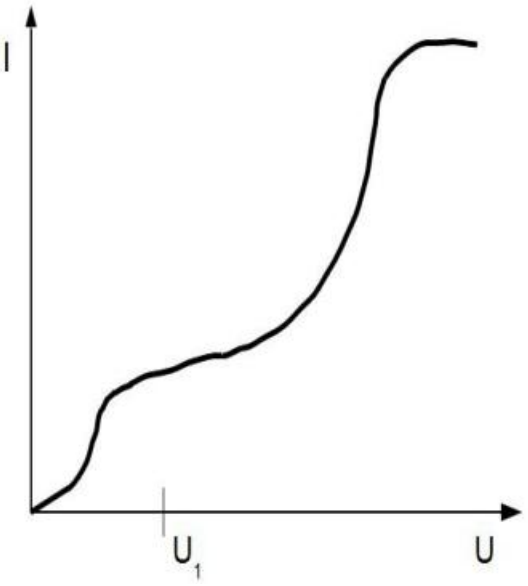


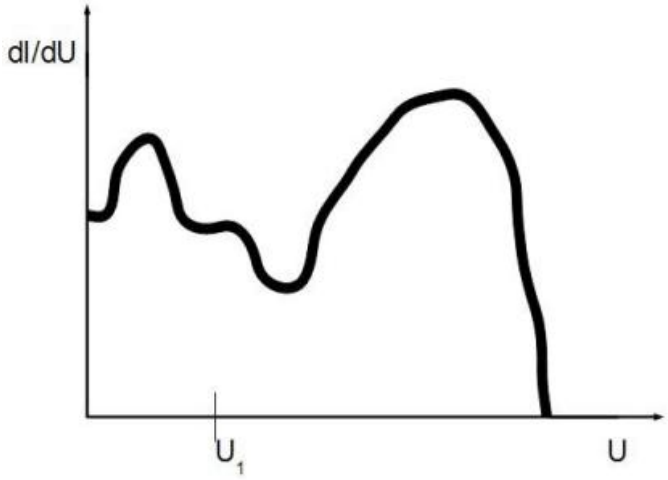

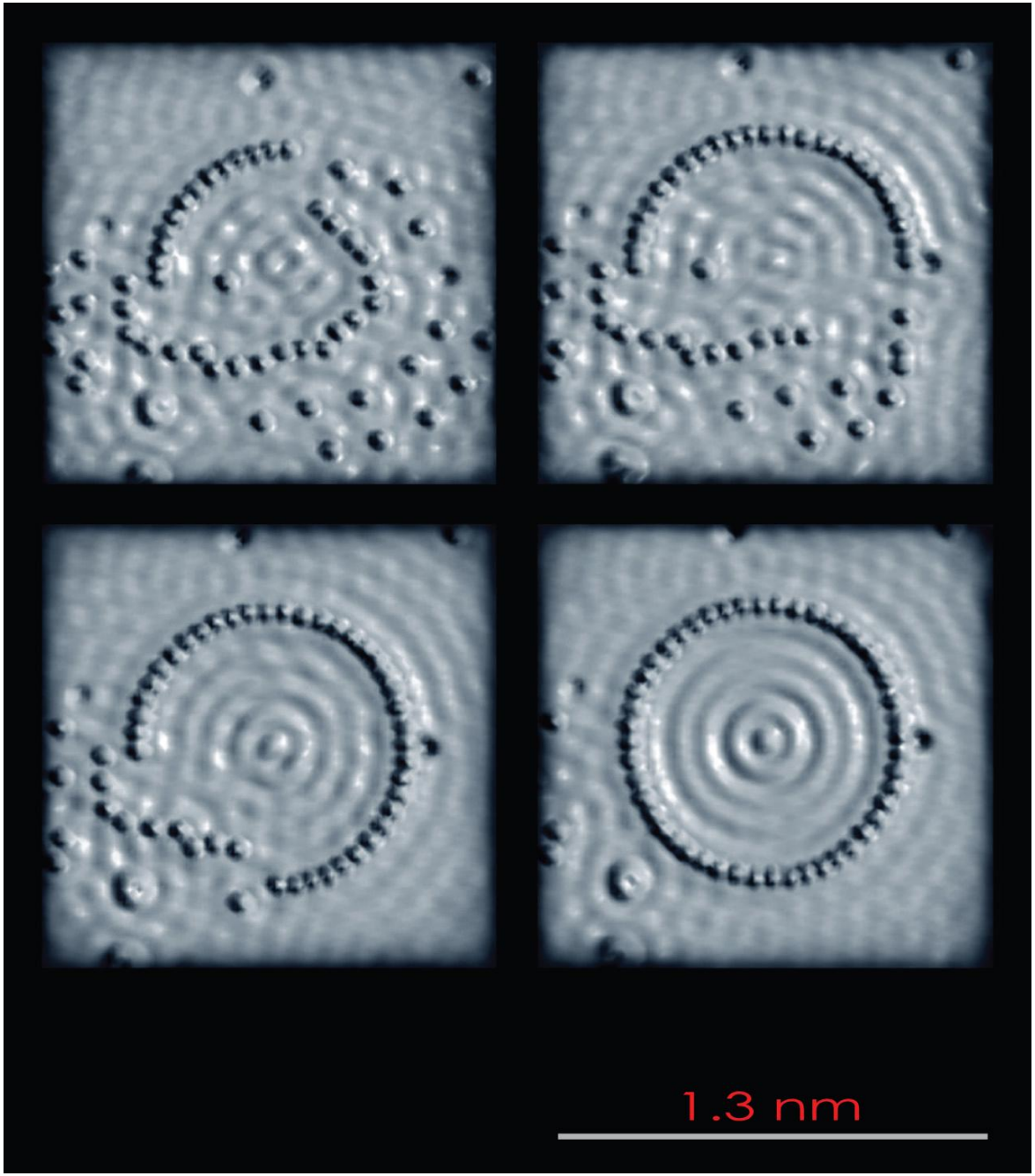
1.3 nm

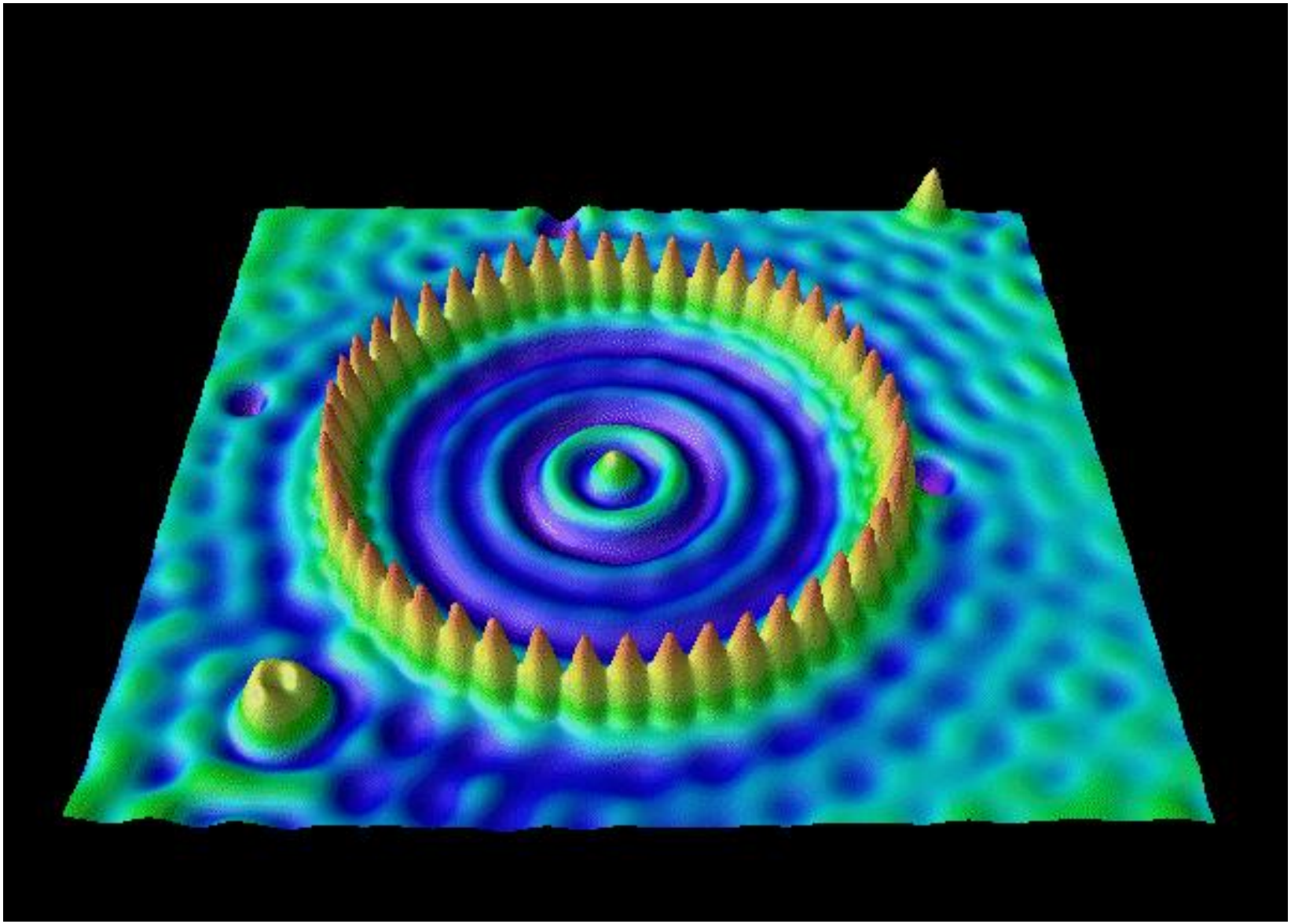

„Quantum Corral“, Fe/Cu(111) (Crommie, Lutz, Eigler 1993), image width 1.3 nm

# Quantenkäfig

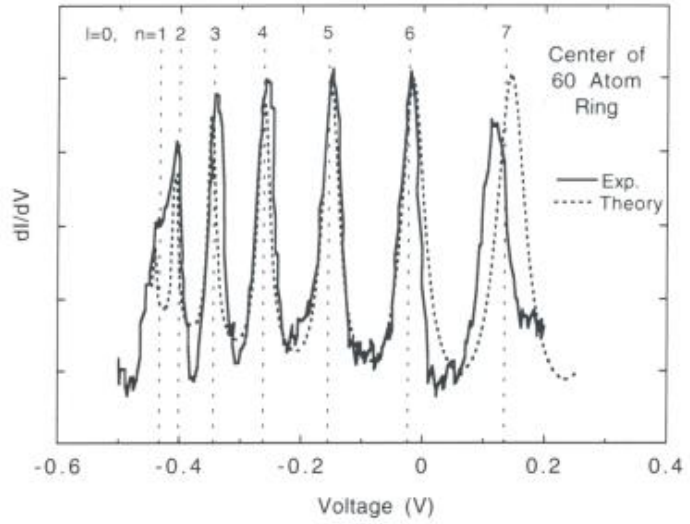


Fig. 9. Solid curve: $dI/dV$ spectrum taken with the STM tip held stationary over the center of the 60 atom Fe ring. The experimental curve has had a smooth background removed. Broken curve: results of multiple-scattering calculation performed in the "black dot" limit (the offset and normalization of the theoretical curve are treated here as free parameters). Vertical lines: theoretical eigenenergies for $l = 0$ states of a round, 2D hard-wall box having the same dimensions as the 60 atom Fe ring.

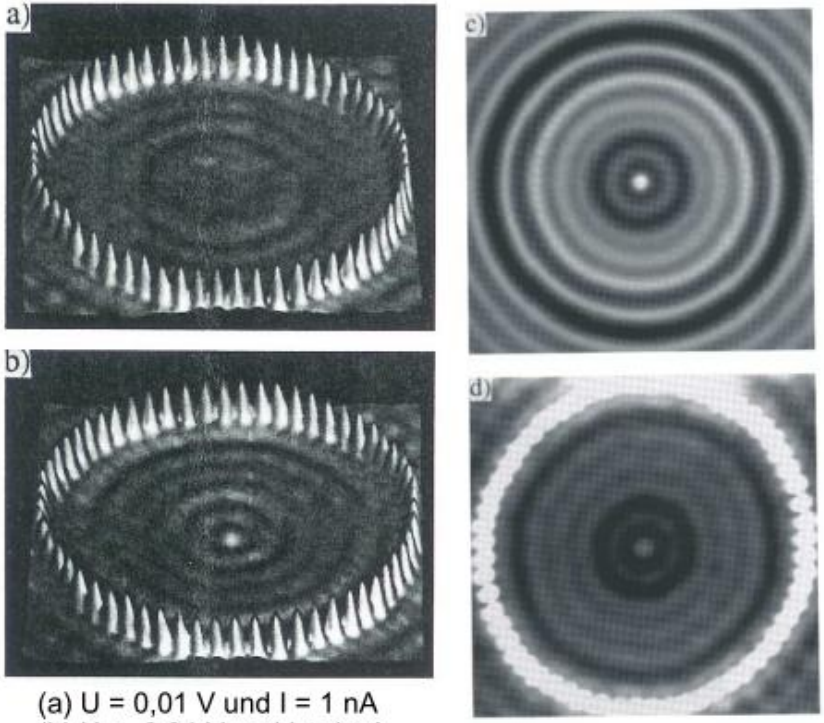


(a) U = 0,01 V und I = 1 nA
(b) U = -0,01 V und I = 1 nA

Aus: Crommie et al., Physica D 83 (1995) 98

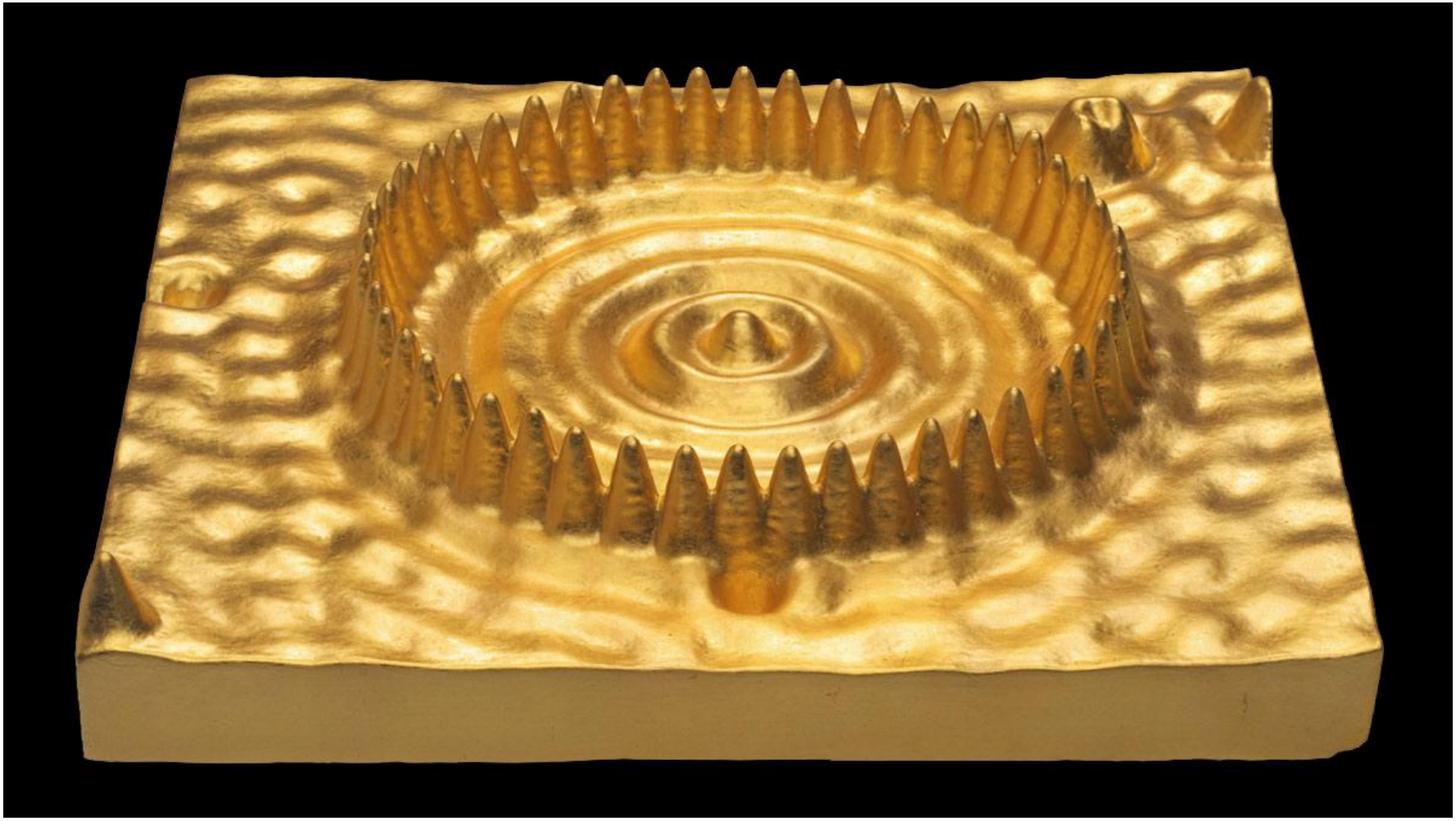

*The Well (Quantum Corral)* (2009) by Julian Voss-Andreae.

Applet for confinement in circular well:

http://www.st-andrews.ac.uk/~qmanim/animations_2/2D_Circular_Well_V2.swf

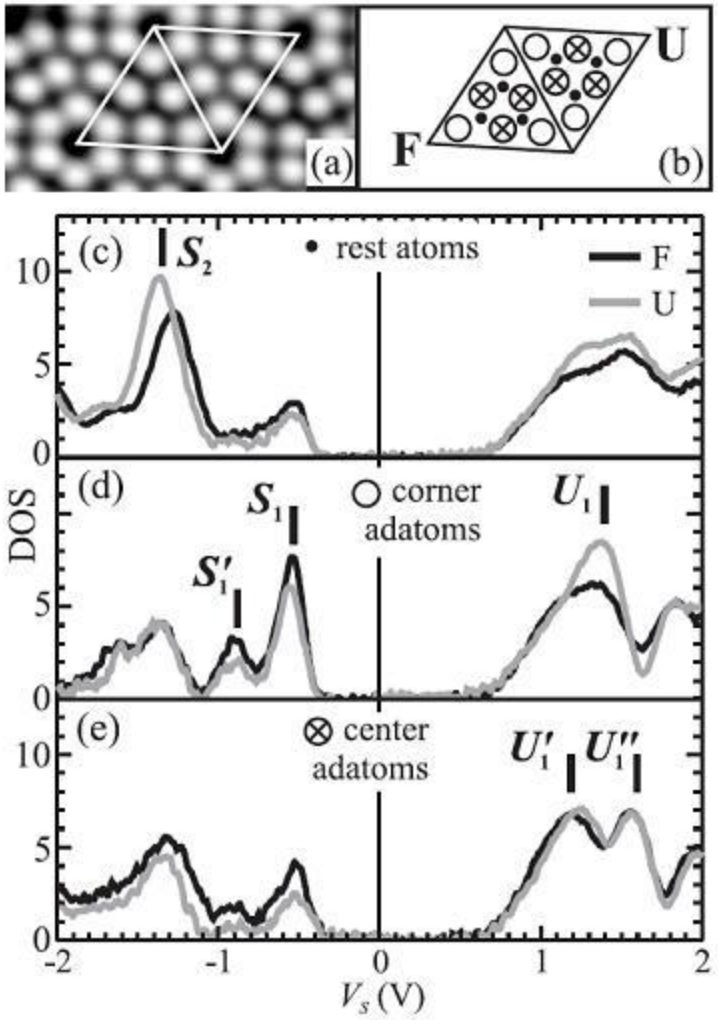


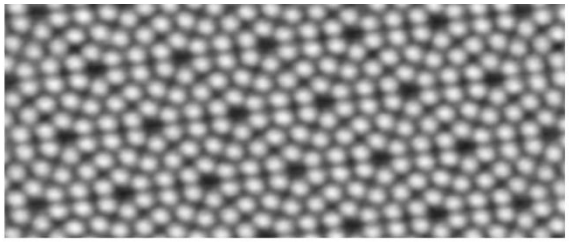

(a)

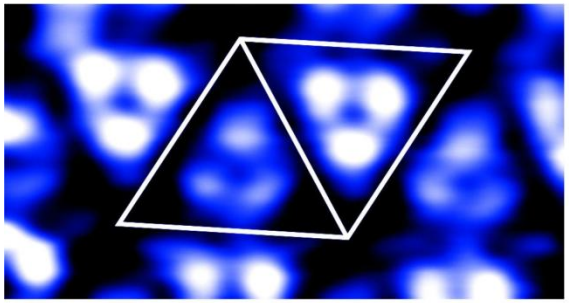

(b) V= -1.3V

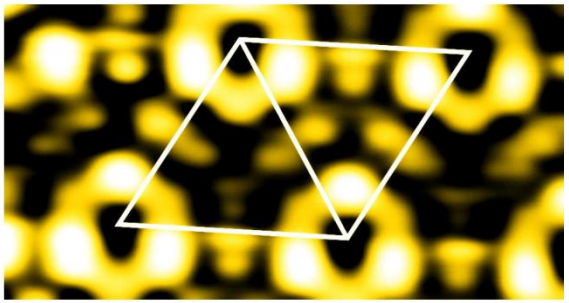

(c) V= -0.5V

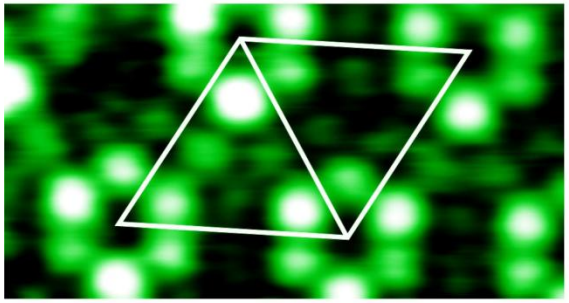

(d) V= 1.4V

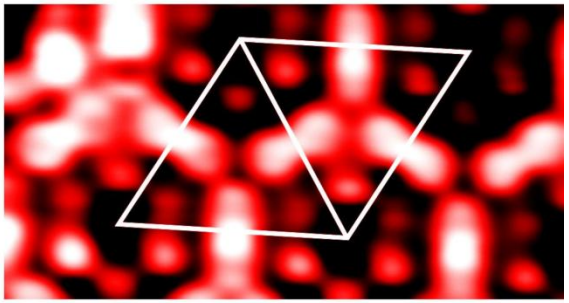

(e) V= 1.6V

# Spin-Polarized STM - Principle

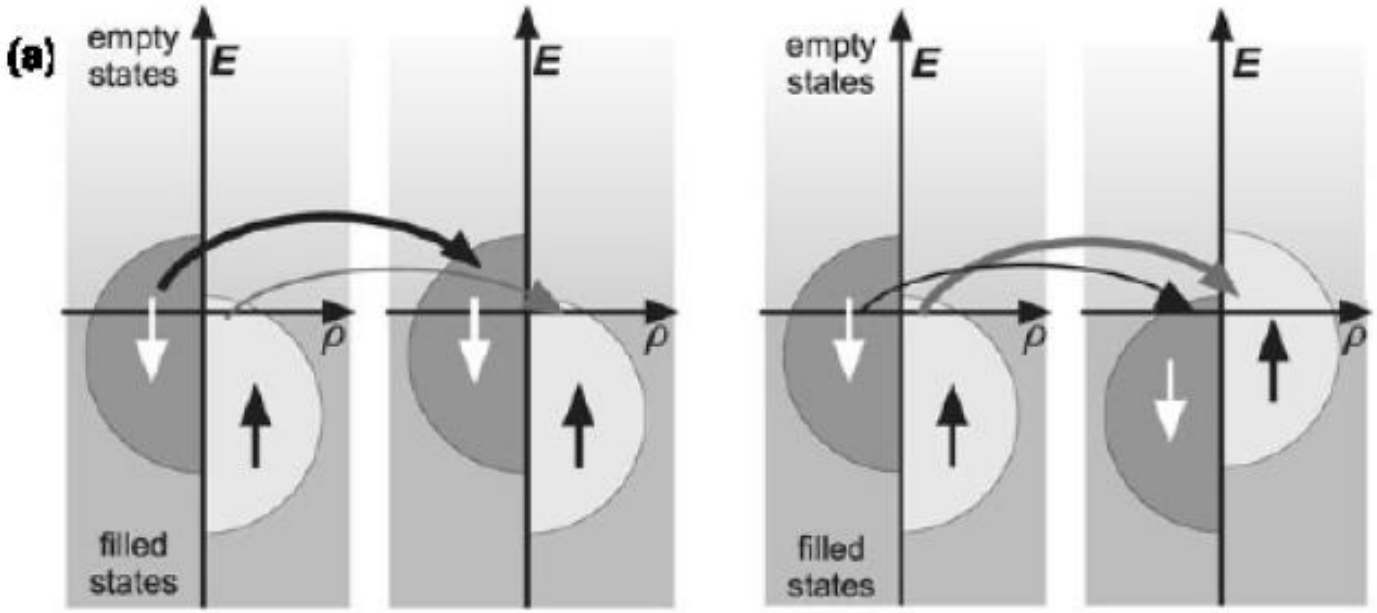


**Figure 2.** Principle of spin-polarized tunnelling between magnetic electrodes that exhibit (*a*) a parallel and (*b*) an antiparallel magnetization. The spin is conserved in the case of elastic electron tunnelling. Therefore, spin-up electrons that tunnel out of the occupied states of electrode A can only enter empty spin-up states of electrode B.

M.Bode, Rep. Prog. Phys. 66 (2003) 523

Fig. 28

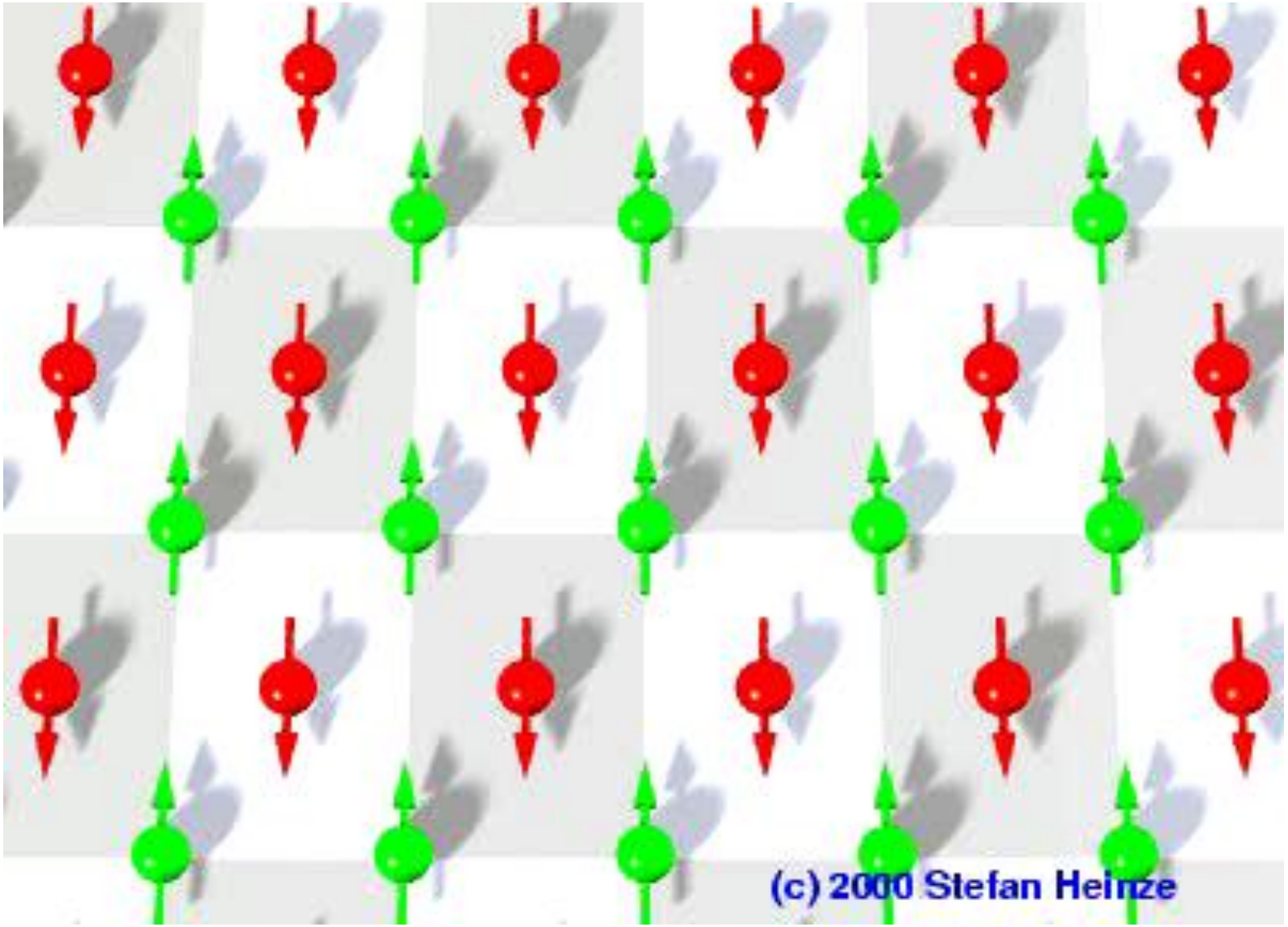
(c) 2000 Stefan Heinze

# Cr(001) as a Topological Antiferromagnet

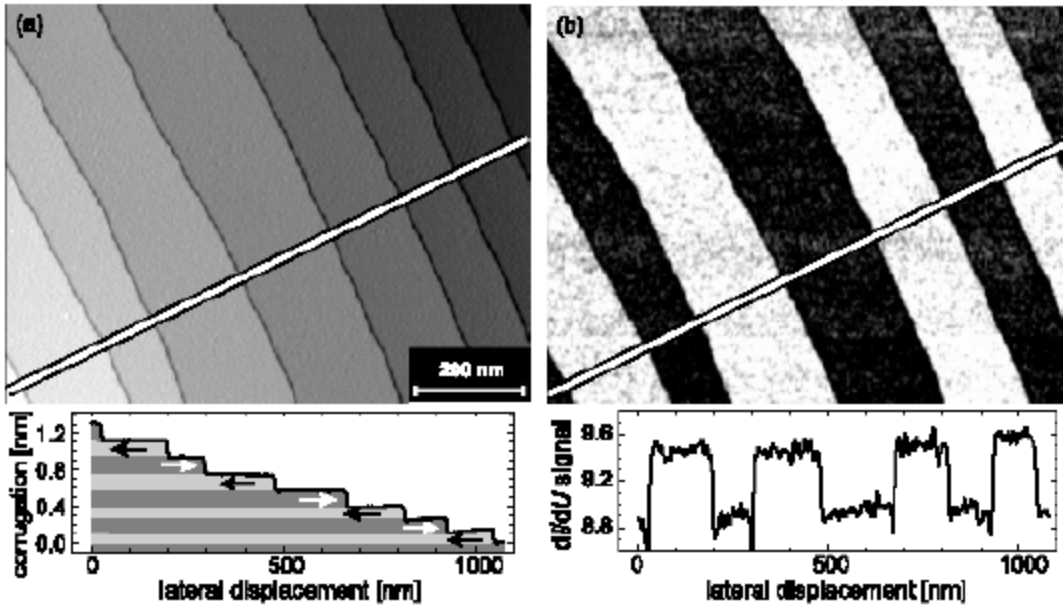


Figure 22. (*a*) Constant-current mode STM image of the Cr(001) surface. Nine te separated by monatomic steps are visible. (*b*) Simultaneously acquired spin-resolved d map at $U = -290$ mV sample bias. The signal changes at every step between low and hig to antiparallel magnetization of adjacent terraces, thereby confirming the model of 'topol antiferromagnetism' proposed by Blügel *et al* [92].

M.Bode, Rep. Prog. Phys. 66 (2003) 52

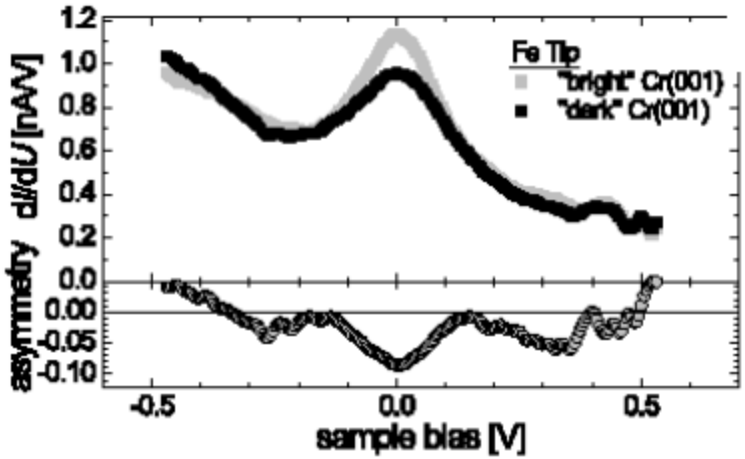


Figure 21. Tunnelling spectra and asymmetry as measured with a Fe coated probe tip above adjacent Cr(001) terraces. The spectra exhibit a peak close to the Fermi level, which is caused by a $d_{z^2}$-like surface state being characteristic for bcc-(001) surfaces [116]. Since the surface state is spin-polarized the intensity depends on the relative orientation of the quantization axes of tip and sample, which—due to the 'topological antiferromagnetism' of Cr(001)—changes between parallel and antiparallel for adjacent Cr terraces.

Fig. 29

# Inelastic Tunneling Spectroscopy (IETS)

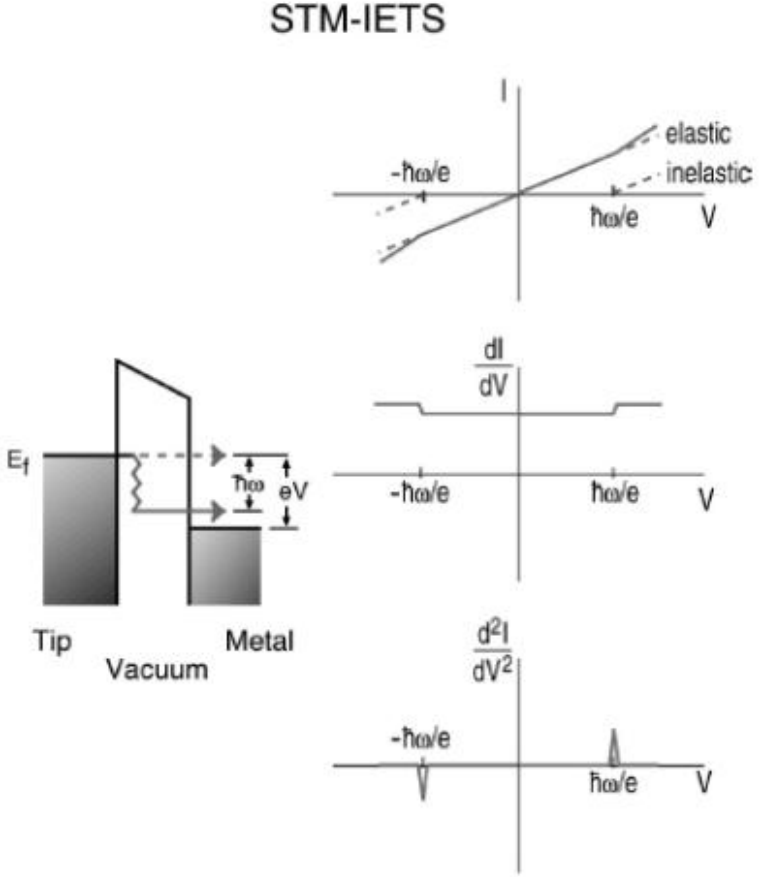


FIG. 3. Schematic showing the emergence of inelastic tunneling at the threshold for vibrational excitation. The change in the tunneling current due to vibrational excitation is too small to be measured from the $I-V$ curve. While a change in the differential conductance, $dI/dV$, can be seen for strong modes, more often vibrational features needs to be extracted from $d^2I/dV^2$. An important characteristic of vibrational inelastic electron tunneling spectroscopy (IETS) is the occurrence of a peak of the opposite sign on the negative bias side. Lacking an isotope shift analysis, the assignment of a feature to vibrational excitation needs to be confirmed by a corresponding feature with the opposite polarity at the opposite bias. This schematic depicts an increase in the conductance, associated with a positive (negative) peak for positive (negative) sample bias. In contrast, electronic spectra arise from elastic tunneling; peaks are positive and occur on either positive (unoccupied states) or negative (occupied states) sample bias.

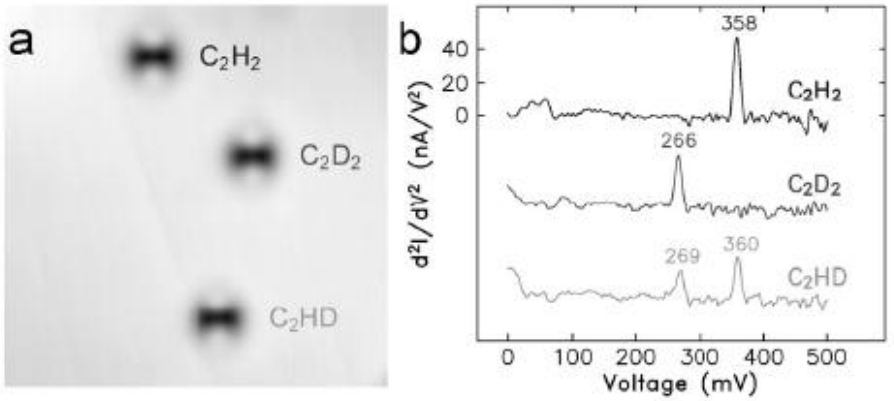


FIG. 4. (a) 56 Å×56 Å STM topographical images and (b) single-molecule vibrational spectra via STM-IETS of three acetylene isotopes on Cu(001) at 8 K. The two protrusions (bright) in the image of each isotope are due to the presence of the C–H and C–D bonds while the central depression (dark) is attributed to the C–C bond. The C–H stretch is observed at 358 meV for $C_2H_2$ and the C–D stretch is observed at 266 meV for $C_2D_2$. Small upshifts are found for the C–H and C–D stretches of $C_2HD$. The $C_2HD$ spectrum demonstrated for the first time single bond sensitivity with STM-IETS.

W. Ho, J. Chem. Phys. 117, 11033 (2002

Fig. 30

# Can you really „see“ atoms?

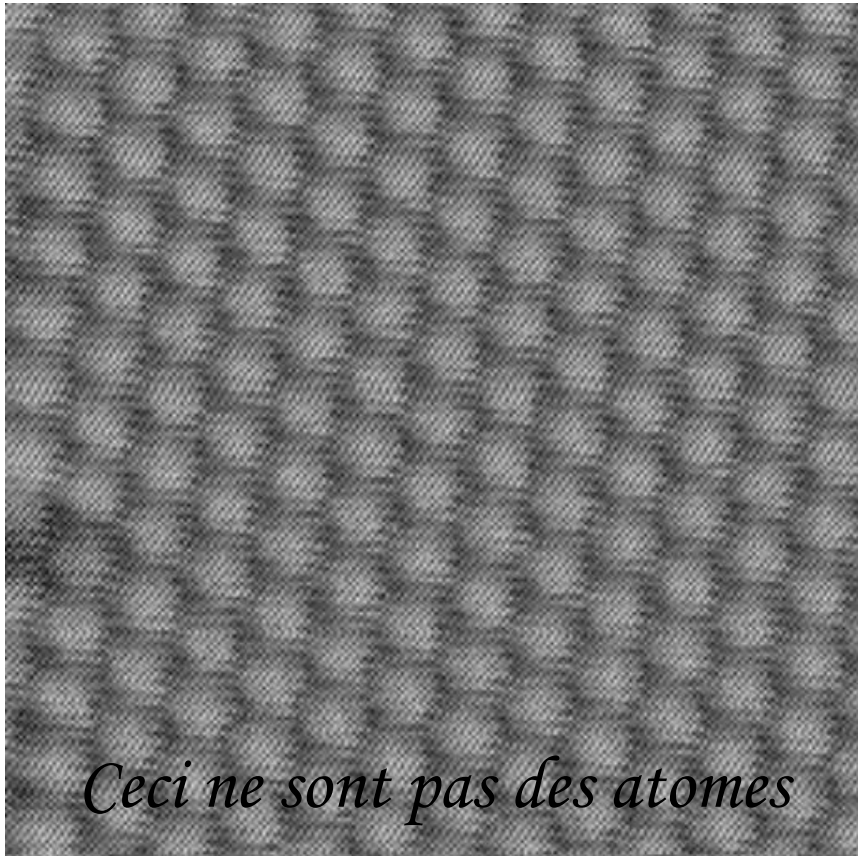


Carsten Busse, 1999 (Al(111))


René Magritte, 1923

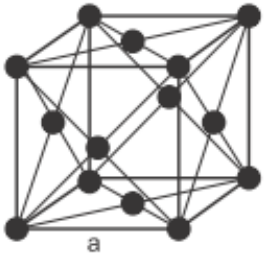


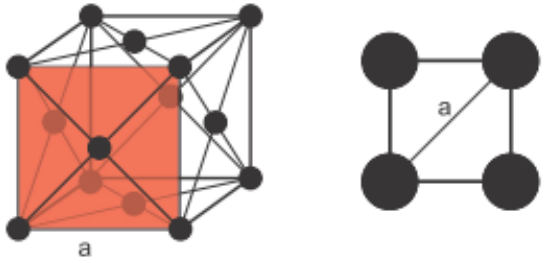


(100)

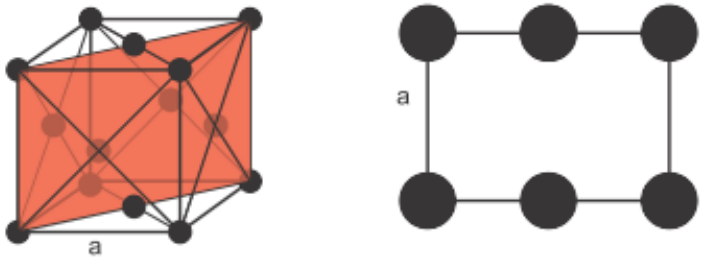


(110)

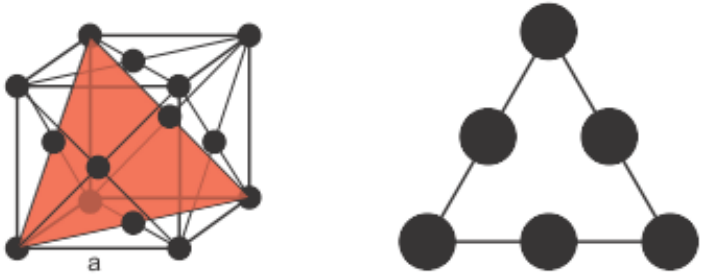


(111)

- was ist denn mit e- - Streuung bei hohen Energien? Kikuchi?
- For neutorns, the crystal really resembles an array of point scatterers
- Vielleicht doch Unterscheidung atomarer Strufaktor unf Formfaktor einführen
- Streudreieck einführen (generell für alle Strahlungen und auf besondere Bedeutung im Fall der Neutronen hinweisen)
- Erklärung der Kleinwinkelstruung über das moiré der Probe-Wave
- Klar daruf hinweisen, dass durch eine Verdoppelung der Einheitszelle keine neuen zwischen den alten entstehen, wir habe vielmehr eine neue, kleiner eZelle im reziproken Raum und einen entsprechenden Formfaktor
- sind diese magnetisch sensitiven NeutronenStreuexperimente of Pulverexperimente?
- XRR?
- vielleicht kleines Maple-Programm zu den Interferenz-Phänomenen? Möglicher gibt es so was ja schon in der Alwimüha
- nicht besprochen: X-Ray microscope
- tolles drehbares Modell von $SrTiO_3$